34th Annual International Conference of the IEEE EMBS
San Diego, California USA, 28 August - 1 September, 2012

Evaluation of Cell Impedance Using a μ-channel

Chia-Hung Dylan Tsai[1], Makoto Kaneko[1] and Fumihito Arai[2]

***Abstract*— We propose a novel approach for evaluating both the stiffness and internal viscosity of a cell by using a μ-channel. The key idea comes from the fact that cell behavior in the channel can be separated into two phases; one is in the entrance area where the cell heavily deforms within a short distance, and the other is in the remaining area where the cell keeps almost constant shape. By focusing on the cell behavior in the first area, we can evaluate the internal viscosity of a cell. By focusing on the cell behavior in the second area, we can evaluate the stiffness. We conducted experiments with two different initial velocities of red blood cells, and discussed the results from the viewpoint of applicability.**

I. Introduction

Cell stiffness is an important index for judging the vitality or activity of cell. For example, red blood cells (RBCs) become stiffer when your body is suffered by Malaria [1]. Also, recent medical report says that RBCs of patients suffered by diabetes become stiffer than those of normal person [2]. As for sensing of the cell stiffness, there are various approaches. The most popular one is perhaps the utilization of AFM (Atomic Force Microscope) [3], where the Young's modulus is computed by the relationship between the deformation of cantilever after making contact with a cell and the displacement of the base of cantilever usually driven by a piezo-actuator. However, for completing the whole procedure, this approach takes time in the order of several minutes at least. On the other hand, there are a couple of works where a high speed camera is utilized for capturing cells motion in narrow channel whose width is less than the diameter of the cell [4] [5]. These approaches are based on the idea that the passing time of a narrow channel depending upon the cell stiffness.

While there have been a number of works for evaluating the cell stiffness, there have been few works evaluating the cell internal viscosity. This is simply due to the difficulty of measurement. The challenge of this paper is to evaluate both stiffness and internal viscosity of cells. Rather than measuring the exact value of stiffness and viscosity, the "evaluation" in this paper is aimed to distinguish the cell stiffness or viscosity between normal and infected cells. The key idea comes from the observed fact that cell behavior in the channel can be separated into two phases as shown in Fig. 1; one is around the entrance area where the cell heavily deforms within a short distance and the other is in the remaining area where the cell keeps almost constant shape. It is observed that the velocity of cells always reach to a constant value in Phase II under the same initial velocity. Since only the stiffness is in effect in this phase, we can evaluate the stiffness by focusing on the velocity value. We also observed that cells exhibit velocity drop before entering the channel in Phase I. The velocity drop is due to the effect of both stiffness and internal viscosity. By focusing on the amount of drop with consideration of the stiffness evaluated from Phase II we can evaluate the internal viscosity of the cell .

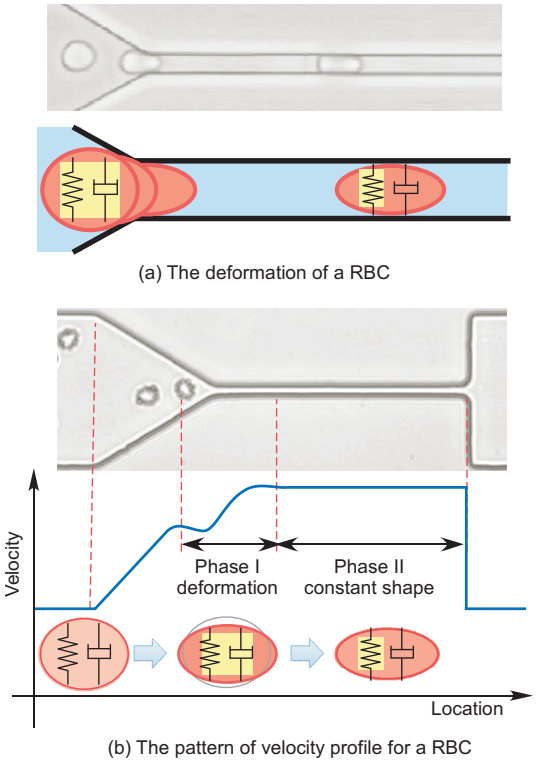

Fig. 1. The deformation of a RBC passing through a μ-channel. Two mechanical elements, a spring and a damper, are used to represent the stiffness and internal viscosity of the cell. The highlight of the element shows the effective element(s). (a) A microscope image and an illustration of a RBC passing through a μ-channel are presented. (b) Two phases of a cell passing through a μ-channel are defined as the phase of deformation and the phase of constant shape.

This paper is organized as follows. After briefly reviewing related works in section II, we explain the basic working idea for evaluating viscosity as well as stiffness in section III, and both experimental system and results in section IV. Then, we discuss the experimental results in section V before concluding remarks in section VI.

[1]C. D. Tsai and M. Kaneko are with the Department of Mechanical Engineering, Osaka University, Osaka, Japan tsai at hh.mech.eng.osaka-u.ac.jp, mk at mech.eng.osaka-u.ac.jp

[2]F. Arai is with the Department of Mechanical Science & Engineering, Nagoya University, Nagoya, Japan arai at mech.nagoya-u.ac.jp

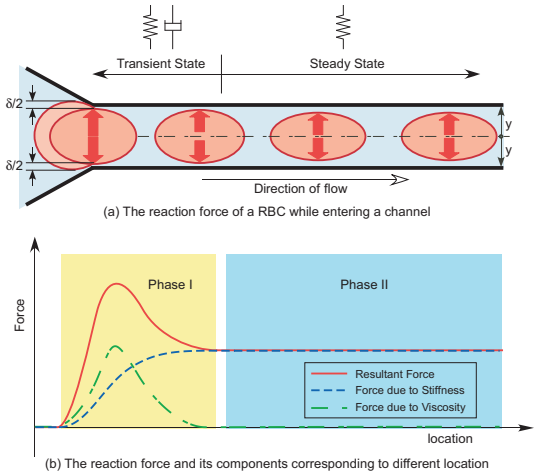

Fig. 2. This figure illustrates the transformation of a RBC from a transient state to a steady state.

II. Related Works

There are two approaches for measuring stiffness of the object; one is direct method [6] where the stiffness is directly evaluated by measuring both contact force and deformation of object, and the other is indirect method [7] [8] where the stiffness is indirectly evaluated, such as by observing the behavior of object without measuring the force imparted to the object. Evaluation through natural frequency or motion observation of object belongs to this approach. Our approach in this paper is categorized into the indirect method. Compared with any direct method, an indirect method enables us to evaluate the stiffness with a shorter time in general.

The viscoelastic property of bio-tissue has been studied from different approaches. For example, Fung studied mechanical properties of living tissues from both the viewpoints of solid mechanics and thermodynamics [9]. As for a high speed vision, Ishikawa and Ishii are pioneers for designing the software as well as the hardware [10] [11]. In order to reduce the computation burden, they propose a window based approach where they focus on a small searching area including the target object. This idea is based on the fact that the object movement should be small enough to ensure the object being always within the window when we increase the frame rate. Ishikawa and Ishii applied the technique for various fields, such as high speed robots, virtual instruments, games, and sensing and control of micro living thing under microscopic capturing. As shown in the above works, a high speed vision should be a kernel technology to detect the object moving in a high speed.

III. Key Idea

a) The effect of stiffness and internal viscosity: The key idea of this paper is as illustrated in Figs. 2 and 3. The arrows in Fig. 2(a) signify the reaction forces by a compressed RBC while entering a μ-channel. The RBC is modeled by two mechanical elements, a spring and a damper, for representing the stiffness and internal viscosity, respectively. The RBC is deformed from its original shape to a shape with a smaller

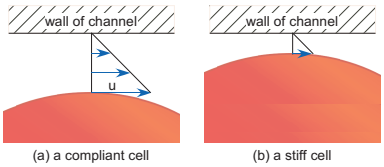

Fig. 3. This figure illustrates the relation between the stiffness and velocity of a cell in a steady state (Phase II).

size in vertical direction in order to squeeze into the μ-channel. The resultant of reactions by a compressed RBC can be expressed as

$$F_r = c\dot{\delta} + k\delta \tag{1}$$

where F_r is the resultant of reactions, δ is the amount of compression in vertical direction, c is the coefficient of the damper and k is the spring constant. Figure 2(b) illustrates the reactions due to the spring and damper at different location. When the cell is in transient state (Phase I), both the spring and damper react to the deformation ($\delta \neq 0$, $\dot{\delta} \neq 0$). When the cell reaches a steady state (Phase II), only the spring contributes to the reaction force ($\delta \neq 0$, $\dot{\delta} = 0$). Since the effect of internal viscosity is not effective in Phase II, we can evaluate the stiffness of a RBC according to its behavior in this phase. By incorporating the stiffness evaluated in Phase II, we can further evaluate the internal viscosity based on the velocity profile in Phase I.

b) The relationship between velocity and stiffness: In the experimental results presented in section IV-B, it is observed that the velocity of a RBC would eventually reach an equilibrium value. The net force acting on the RBC must be zero at the moment, and it can be expressed as

$$\sum F = \Delta P(\pi R^2) - \tau(2\pi RL) = 0 \tag{2}$$

where ΔP is the pressure difference, R is the radius of the cross-sectional area of the channel, τ is the shear stress and L is the length of the cell along the direction of motion. The first term in (2) represents the force pushing the cell forward due to the pressure difference, while the second term represents the resisting force due to the viscosity of the fluid. By employing the equation of Newtonian fluid[1], we can have

$$\frac{du}{dy} = \frac{\Delta PR}{2\mu L} \tag{3}$$

where μ is the viscosity of the fluid, du/dy is the velocity gradient, u and y are the flow rate of the fluid and the distance from the center line, respectively. Eq. (3) shows that the velocity gradient would be the same if the cell length is the same, and the conditions of experiment are fixed. Assuming the compressing force by the channel wall is constant, a low-stiffness cell would deform more comparing to a high-stiffness cell, and it leads to different sizes of gaps between the cell and the channel wall as illustrated in Fig. 3. As a result, the velocity of a compliant cell would have a relatively

[1]The Reynolds number of a RBC in saline solution is reported in the range of $1.2-3.5\times10^{-2}$ [12], so that the inertia effect of the RBC is small enough to be neglected.

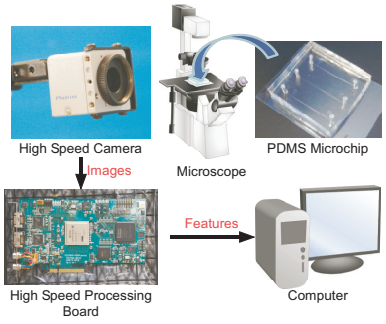

Fig. 4. The experimental setup includes a silicone chip with μ-channels, a microscope, a high speed camera, a high speed processing board and a computer.

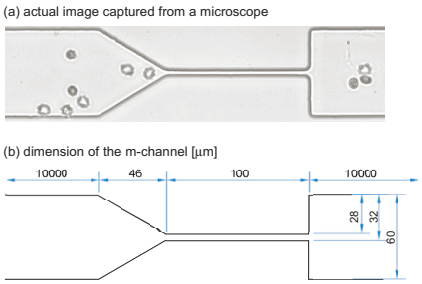

Fig. 5. (a) An actual image of the μ-channel used in the experiment is captured by the experimental setup shown in Fig. 4. (b) This figure shows the design and dimension of the μ-channel with the unit in μm.

large value comparing to the velocity of a stiff cell in Phase II.

IV. Experiment

A. Experimental Setup

The experiments were conducted on the experimental setup shown in Fig. 4. A microscope is equipped with a high speed vision system. The shutter speed and the spatial resolution of the system are set to $1ms$ and $0.506\mu m$, respectively. A PDMS μ-chip was fabricated with a μ-channel inside it. The dimension of the channel is 100 μm in length, 4 μm in height and 4 μm in width, as shown in Fig. 5. The RBCs from human subjects were used for the experiments. The RBCs have an average diameter of 6 μm. The velocity of the flow inside the channel was controlled by adjusting the pressure difference between the pressure at inlet and the outlet of the μ-channel. When the pressure difference increases, it results in the increase of the flow rate, and vice versa. We defined the initial velocity u_0 as the velocity of RBCs when they are in the area with the width of $60\mu m$. Two different pressure difference were employed in the experiments. The initial velocities were measured experimentally, and were $0.033\mu m/ms$ and $0.20\mu m/ms$.

The experimental procedure is described as follows:

1) First, saline water was injected into the μ-channel to make sure there is no air in the channel, so the RBCs can freely flowing inside. The RBCs is then injected into the μ-channel for the test.
2) The velocities of the RBCs inside the channel were monitored by a real-time program with the high-speed vision system. Once the velocity achieves the value of interest, the high speed vision system will start recording the images focusing on the μ-channel with the prescribed shutter speed.
3) After finishing capturing the images from the high-speed vision system, the images were processed by a computer for tracking the trajectory of the RBCs to get the information of the location of RBCs. The velocity values were then calculated by differentiating the tracked locations with respect to the time.

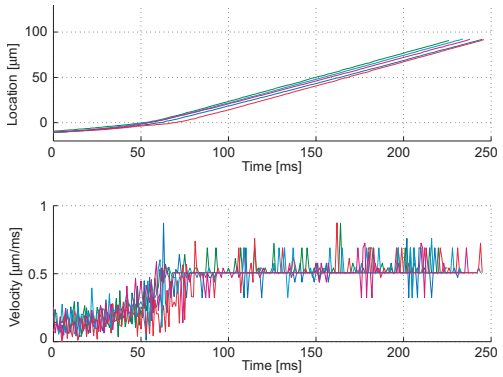

Fig. 6. The plots of the location versus time and the velocity versus time is shown in the upper half figure and the lower half figure, respectively. The average initial velocity u_0 in this set of data is 0.033 $\mu m/ms$

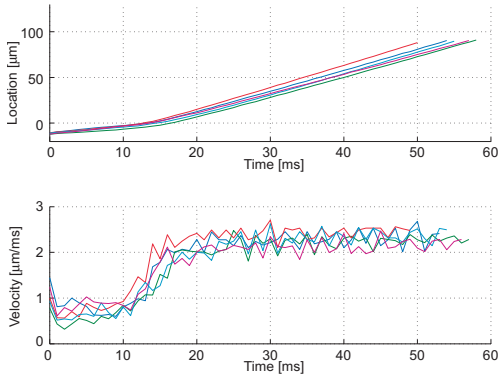

Fig. 7. The plots of the location versus time and the velocity versus time is shown in the upper half figure and the lower half figure, respectively. The average initial velocity u_0 in this set of data is 0.21 $\mu m/ms$

B. Experimental Results

The experimental results with different initial velocities are presented in Figs. 6 and 7. Figures. 6(a) and 7(a) shows the relation between the location and the time of the RBCs. The tracked locations represent the centroid of the RBCs in the captured images. The location is calibrated as zero at the entrance point of the μ-channel. The results of velocity versus time are presented in Figures. 6(b) and 7(b).

The results were plotted as velocity versus location in Fig. 8(b). Figure 8(a) shows an example of the captured image at the moment when a RBC was detected in front of the entrance. The dashed lines in Fig. 8 indicate the corresponding location of the plot with the actual location in the channel.

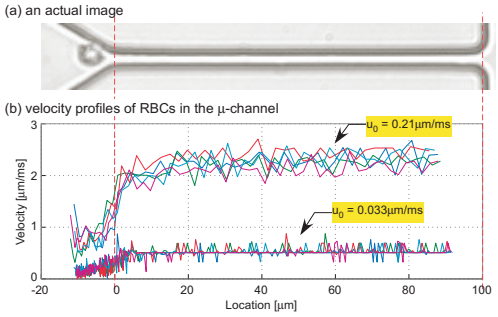

Fig. 8. (a) a snapshot of a cell before entering the μ-channel. (b) Two sets of experimental results with different initial velocities, $u_0 = 0.033\mu m/ms$ and $u_0 = 0.21\mu m/ms$, are presented in the plot of velocity versus location.

V. Discussions

A. *Evaluation of stiffness* – the velocity in Phase II

From the experimental results, both profiles show that the velocities become constant values in Phase II. According to (1), when the shape of a compressed cell is constant, $\dot{x} = 0$, the damper is no longer in effect but only the stiffness. Therefore, the stiffness can then be evaluated by the value of the velocity in this phase. For example, a RBC is stiffer comparing to another when the velocity of it in Phase II is a slower. Conversely, if the velocity is faster, it means a more compliant RBC.

B. *Evaluation of internal viscosity* – the velocity drop in Phase I

In Phase I, the RBCs were deformed due to the fluid pressure and the constraint of the walls. Both the stiffness and the internal viscosity of the cell are in effect. We observed that the velocity of the RBCs had a drop before fully entered the channel. The drop with $u_0 = 0.21\mu m/ms$ is more significant than the one with $u_0 = 0.033\mu m/ms$. It is believed that this phenomenon is due to the internal viscosity of the cell. For the same amount of compression of a RBC to squeeze into the channel, the high initial velocity leads to a high strain rate, and the low initial velocity causes a low strain rate. It can also be explained by (1), the viscosity effect will be more significant with a high strain rate, $\dot{x}$. The hypothesis is confirmed with the phenomenon of *the velocity drop* observed in the experimental results. On the other hand, if we fix the initial velocity of RBCs with different internal viscosities. It is reasonable to expect that the RBCs with a greater internal viscosity to have a more significant *velocity drop* than the RBCs with a lower internal viscosity.

C. *Velocity profile for the examination of cell condition*

Two significant phenomena, *velocity drop in Phase I* and *constant velocity in Phase II*, of the velocity pattern have been observed and discussed in this paper. The value of constant velocity in Phase II and the amount of velocity drop in Phase I can be used as two indexes for examining the impedance of cells in practice. For example, we can tell the difference of stiffness from one cell to another if the velocities in Phase II are different. Also, we can find the difference of internal viscosity by different amount of velocity drops in Phase I. With these two indexes, we provide a new way to diagnose diseases which cause the change of RBC properties.

VI. Concluding Remarks

A new approach for evaluating the stiffness and internal viscosity of a cell is presented with experimental results. The velocity profile has been found showing the same pattern consistently among different RBCs. The motion of a RBC inside a μ-channel can be separated into two phases: Phase I, *the phase of deformation* and Phase II, *the phase of constant shape*. The stiffness of a cell can be evaluated by the equilibrium velocity in Phase II, while the internal viscosity of a cell can be evaluated by the *velocity drop* in Phase I. The proposed methodology provides a new way to evaluate the characteristics of cells, and has a great potential in improving the diagnosis of RBC-related diseases.

VII. Acknowledgement

This work is supported by The Ministry of Education, Culture, Sports, Science and Technology (MEXT) of Japan Grant-in-Aid for Scientific Research on Innovative Areas “Bio Assembler”.

References

[1] F. K. Glenister, R. L. Coppel, A. F. Cowman, N. Mohandas, and B. M. Cooke. Contribution of parasite proteins to altered mechanical properties of malaria-infected red blood cells. *Blood*, 99(3):1060–1063, 2002.

[2] K. Tsukada, E. Sekizuka, C. Oshio, and H. Minamitani. Direct measurement of erythrocyte deformability in diabetes mellitus with a transparent microchannel capillary model and high-speed video camera system. *Microvascular Research*, 61:231–239, 2001.

[3] G. Binnig, C. F. Quate, and C. Gerber. Atomic force microscope. *Physical Review Letters*, 56(9):930–933, 1986. AFM1.

[4] Y. Imamura, T. Tajikawa, K. Ohba, and T. Takubo. Measurement of the time constant of shape recovery of human erythrocyte using a micro-channel technique. *Mechanical Engineering Congress 2009*, 6(09-1):197–198, 2009.

[5] Y. Hirose, K. Tadakuma, M. Higashimori, T. Arai, M. Kaneko, R. Iitsuka, Y. Yamanishi, and F. Arai. A new stiffness evaluation toward high speed cell sorter. In *Proc. of the IEEE Int. Conf. on Robotics and Automation (ICRA)*, pages 4113–4118, Anchorage, USA, May 2010.

[6] N. Tanaka, M. Higashimori, and M. Kaneko. Active sensing for viscoelastic tissue with coupling effect. In *30th Annual Int. Conf. of the IEEE Engineering in Medicine and Biology Society (EMBC)*, pages 106–111, Vancouver, Canada, Aug 2008.

[7] M. Kaneko, C. Toya, and M. Okajima. Active strobe imager for visualizing dynamic behavior of tumors. In *Proc. of the 2007 IEEE International Conf. on Robotics and Automation*, pages 2009–2014, 2007.

[8] M. Kaneko, N. Kanayama, and T. Tsuji. Active antenna for contact sensing. In *Proc. of the 2007 IEEE International Conf. on Robotics and Automation*, pages 278–291, 1998.

[9] Y. C. Fung. *Biomechanics: Mechanical Properties of Living Tissues*. Springer-Verlag, 1993.

[10] T. Komuro, I. Ishii, M. Ishikawa, and A. Yoshida. A digital vision chip specialized for high-speed target tracking. *IEEE Trans. Electron. Devices*, 50:191–199, 2003.

[11] K. Tajima, A. Numata, and I. Ishii. Development of a high- resolution, high-speed vision system using cmos image sensor technology enhanced by intelligent pixel selection technique. In *Optics Ea 2004, Proc. SPIE*, volume 5603, pages 215–224, 2004.

[12] Y. Sugii, R. Okuda, K. Okamoto, and H. Madarame. Velocity measurement of both red blood cells and plasma of in vitro blood flow using high-speed micro piv technique. *Measurement Science and Technology*, 16:1126–1130, 2005.